RSC Sustainability

ROYAL SOCIETY OF CHEMISTRY

PAPER

View Article Online
View Journal | View Issue

Cite this: *RSC Sustainability*, 2025, **3**, 5632

A green strategy for treating nitrate-contaminated wastewater using a zeolite P-based composite derived from rice husk ash

Nhu-Y Nguyen-Thi, *[a] Yen Nhi Nguyen-Thi,[a] Cuong-Quoc Nguyen, [b] Kim-Phung Ly,[c] Nguyen Minh Nhut,[d] Luong Huynh Vu Thanh,[d] Quang Le Dang,[ef] Quang De Tran [b] and Phuong Lan Tran-Nguyen[g]

Pollution of aquatic environments by nitrate ions has become increasingly severe in recent years. Specifically, nitrate contamination in aquaculture and seafood processing wastewater is an urgent environmental challenge, as excessive nitrate discharge can trigger eutrophication, degrade water quality, and threaten both aquatic ecosystems and human health. Developing low-cost and sustainable adsorbents is therefore essential for effective nitrate management, especially in regions like the Mekong Delta where rice husk ash is abundant. Rice husk ash, an agricultural by-product, is a promising raw material for synthesizing zeolite and zeolite-based composites which have gained attention for their enhanced adsorption ability. To solve nitrate pollution and utilize rice husk ash, a chitosan/zeolite NaP1 composite was developed using zeolite NaP1 synthesized from rice husk ash. The composite was prepared with a chitosan : zeolite NaP1 weight ratio of 1 : 2 (w/w), glutaraldehyde 4%, and a mixing time of 1 h. The composite showed an optimal adsorption efficiency and adsorption capacity of 58.47% and 70.83 mg g^{-1}, respectively at pH 5, an adsorbent dose of 1 g L^{-1}, and a nitrate concentration of 100 mg L^{-1} in 30 min. Experimental data fitted both Langmuir and Freundlich adsorption isotherm models well, with a high maximum capacityof 107.761 mg g^{-1} from the Langmuir model whereas pseudo-first-order and pseudo-second-order kinetics also described the process well. The composite exhibited good reusability, confirming its potential for sustainable application towards wastewater treatment.

Received 17th July 2025
Accepted 23rd September 2025

DOI: 10.1039/d5su00593k

rsc.li/rscsus

Sustainability spotlight

This research addresses nitrate pollution through the sustainable synthesis of a chitosan/zeolite NaP1 (CZP) composite derived from rice husk ash, a widely available agricultural by-product. By converting waste into effective nitrate adsorbents, the study promotes circular economy principles and significantly enhances wastewater treatment, aligning with UN Sustainable Development Goals, specifically SDG 6 (Clean Water and Sanitation) and SDG 12 (Responsible Consumption and Production). The developed CZP composite demonstrates high adsorption efficiency, good reusability, and environmentally friendly production, thus contributing positively towards the reduction of eutrophication, protecting aquatic ecosystems, and supporting sustainable resource management in industries like seafood processing and agriculture.

1. Introduction

Nowadays, the intrusion of pollutants into aquatic environments has become increasingly severe, specifically phosphate and nitrate.[1,2] Agricultural and industrial activities are among the most common sources of water pollution.[3] The side effects of agricultural practices, namely residual pesticides or fertilizers, are harmful to water bodies, as the excess amounts can infiltrate into soil, lakes, and groundwater, thus causing contamination. More seriously, high concentration nitrate-contaminated wastewater from seafood processing plants needs to be treated on-site in an effective and environmentally friendly manner before being discharged into the environment.

[a]*Faculty of Biological, Chemical, and Food Technology, Can Tho University of Technology, Can Tho 94000, Vietnam. E-mail: ntny@ctuet.edu.vn; Tel: +84-909-163-385*
[b]*Department of Health Sciences, College of Natural Sciences, Can Tho University, Can Tho 94000, Vietnam*
[c]*Stem Cell Laboratory, Department of Molecular Biology, Institute of Biotechnology and Food, Can Tho University, Can Tho 94000, Vietnam*
[d]*Faculty of Chemical Engineering, College of Engineering, Can Tho University, Can Tho 94000, Vietnam*
[e]*Institute of Materials Science, Vietnam Academy of Science and Technology (VAST), 18 Hoang Quoc Viet, Hanoi, Vietnam*
[f]*Graduate University of Science and Technology, Vietnam Academy of Science and Technology (VAST), 18 Hoang Quoc Viet, Hanoi, Vietnam*
[g]*Faculty of Mechanical Engineering, College of Engineering, Can Tho University, Can Tho 94000, Vietnam*

Vietnam ranks among the world's leading seafood and aquatic product exporters.[4–6] In 2024, the total aquaculture area was estimated to reach 1.3 million hectares of inland farming and 9.7 million m^3 of marine cage farming (Fig. S1 in SI).[7] Throughout the aquaculture and seafood processing, a large amount of organic waste is released into the environment daily. These wastes undergo microbial decomposition, resulting in the accumulation of nitrates in aquaculture wastewater (Fig. 1). In addition, nitrate-rich seafood processing wastewater, if discharged directly into surrounding ecosystems, poses potential risks to environmental quality and ecological balance. High nitrate concentrations lead to algal blooms, which adversely affect the habitats of aquatic organisms and humans (Fig. S2 in SI).[8] To address this situation, adsorption was considered one of the most promising solutions due to its simplicity and low cost.[3] The selection of an appropriate adsorbent with a high adsorption capacity (AC) is a considerable interest.

In recent research, we have successfully utilized lignin extracted from sugarcane bagasse for the treatment of wastewater contaminated with dyes and heavy metals. The study highlights the applicability of agricultural by-products in environmental remediation and promotes the advancement of green chemistry.[9] Zeolites, widely recognized for their good AC, can be synthesized from various sources, including commercial sources, agricultural or industrial by-products and natural minerals.[10] Among these, by-products have gained the most interest due to their availability and low cost. Rice husk ash (RHA), a common by-product with large reserves in the Mekong Delta, contains silica as the major component, which can be used as a raw material for zeolite synthesis.[10] However, the application of zeolites in wastewater treatment is hindered by the difficulty in recovering the adsorbent after use, due to their small particle sizes. As a result, combining zeolites with other types of adsorbents has been investigated. Chitosan, a product of chitin deacetylation, is non-toxic to the environment.[11] Due to the presence of active –OH and $–NH_2$ groups in the structure of chitosan, besides its biomedical applications, chitosan is also used for the treatment of pollutant ions.[12,13] Several previous studies have combined zeolite and chitosan to generate composites;[2,11,13] however, the AC of zeolite/chitosan composites towards nitrate has not been evaluated. This study aims to treat nitrate ions in aqueous solutions using chitosan/zeolite NaP1 (CZP), a material that improves nitrate adsorption efficiency and facilitates post-adsorption material recovery compared to zeolite NaP1 (ZP) and chitosan separately. Effects of composite synthesis factors such as the chitosan-to-ZP mass ratio (C : ZP) and glutaraldehyde concentration on the properties of composite were investigated. Furthermore, the effect of adsorption conditions, including pH, adsorbent dose, nitrate concentration, and contact time was also examined. Moreover, adsorption isotherm models (Langmuir and Freundlich) and kinetic models (pseudo-first-order (PFO) and pseudo-second-order (PSO)) were applied to the experimental data to elucidate the nitrate adsorption mechanism on the composite.

In summary, this study aims not only to propose a practical strategy for water decontamination but also to underscore the broader potential of rice husk as a sustainable and versatile resource for multifaceted environmental applications.

2. Experimental

2.1. Materials

Rice husk ash was collected from Tra Noc Industrial Zone, Can Tho City. Then, large impurities were removed, and RHA was finely ground before use. Chitosan was purchased from a commercial source (90%, Chitosan Vietnam Co., Ltd).

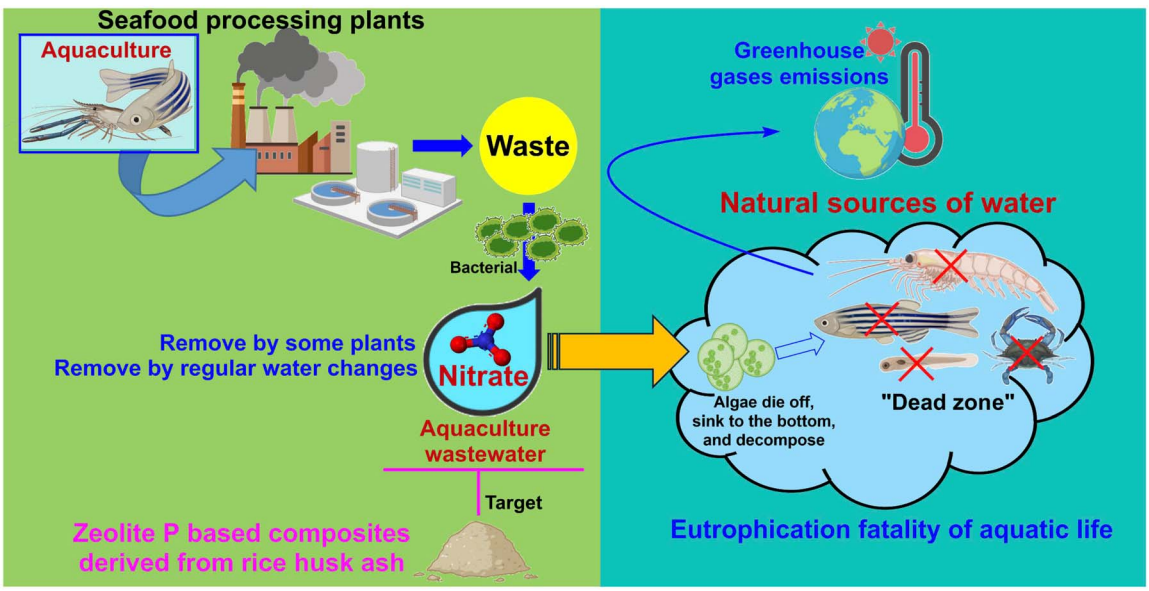

Fig. 1 During aquaculture processes, wastewater is enriched with nitrates derived from organic waste decomposition by microorganisms. Although a portion of these nitrates is removed naturally through uptake by aquatic plants and routine water exchange, significant amounts may persist. The uncontrolled discharge of residual nitrates into natural ecosystems can trigger eutrophication, leading to severe environmental degradation and contributing to the intensification of greenhouse effects.

Chemicals such as sodium hydroxide (NaOH, 96%), acetic acid (CH_3COOH, 99.5%), hydrochloric acid (HCl, 36–38%), sulfuric acid (H_2SO_4, 98%), ethylenediamine tetra acetic acid (EDTA, 99.5%), and potassium chloride (KCl, 99.5%) were supplied from Xilong, China. In addition, some chemicals for the determination of nitrate, including sulfamic acid (H_2NSO_3H, 99.3%) and sodium salicylate ($C_7H_5NaO_3$, 99.5%) were obtained from Merck, USA.

2.2. Synthesis process of the CZP composite

The synthesis process of ZP was carried out based on a previous study.[10] The CZP composite was synthesized according to another study with some modifications.[11] The process included (i) dissolving 1 gram of chitosan in 100 mL of 5% acetic acid solution; (ii) adding an exact amount of ZP to the above mixture with various mass ratios of chitosan : ZP (C : ZP) from 1 : 1–1 : 5 ($g : g$); (iii) adding 25 mL of 1% glutaraldehyde solution into the synthesis system; (iv) stirring for 1 h at room temperature to obtain a homogeneous mixture; and (v) slowly adding the above mixture into 500 mL of 0.5 M NaOH solution to solidify the material. The CZP composite was separated, washed to neutral pH and dried to a constant mass at 60 °C overnight. Table S1 summarizes the factors affecting the properties of the composite investigated in this study.

2.3. Characterization of the material

The properties of ZP, chitosan and CZP composites were characterized by methods such as Fourier transform infrared spectroscopy (FTIR), zeta potential, X-ray diffraction (XRD) and scanning electron microscopy (SEM). The characteristic vibrations of ZP and CZP composites were observed in the wavenumber range from 500 to 4000 cm^{-1} using a Jasco FT/IR 4600, Japan. A nanoParticaSZ-100 (Horiba, Japan) was used to measure the zeta potentials of ZP and CZP composites. The characteristic peaks of ZP and CZP composites were characterized by XRD analysis (D8 diffractometer, Bruker, Germany). The instrument was operated in the 2θ angle scanning range from 10 to 70° at room temperature with CuKα radiation ($\lambda = 1.5406$ Å). The morphology of CZP composites was observed from images provided by using a scanning microscope (S4800, Hitachi, Japan). The isoelectric point of CZP composites was determined by impregnation with KCl solution.[11]

2.4. Evaluation of nitrate adsorption ability using the CZP composite

The nitrate adsorption process was carried out as follows: 0.05 g of the composite was added to 50 mL of nitrate solution (100 mg L^{-1}), and shaken for 30 min at room temperature at a shaking speed of 200 rpm. Then, the composite and the solution were separated by centrifugation (Centrifuge Smart 15 Plus – Hanil, Korea); the nitrate concentrations before and after adsorption were determined according to the method of TCVN 6180:1996.[14] The adsorption efficiency (AE) and AC were calculated based on formulae (1) and (2).

$$\mathrm{AE}(\%) = \frac{C_0 - C_e}{C_0} \times 100 \quad (1)$$

$$\mathrm{AC}\left(\mathrm{mg\ g^{-1}}\right) = \frac{(C_0 - C_e) \times V}{m} \quad (2)$$

The nitrate adsorption ability of the CZP composite under different conditions including pH (4–9), material mass (0.5–2.0 g L^{-1}), nitrate solution concentration (10–180 mg L^{-1}) and contact time (15–720 min) was investigated. The adsorption isotherm (Langmuir and Freundlich) and PFO and PSO kinetic models were used to fit the experimental data and propose mechanisms of nitrate adsorption onto the CZP composite.

2.5. Reusability of the CZP composite

The CZP composite after nitrate adsorption was collected to determine the reusability. The composite after adsorption was desorbed by 0.1 M NaOH solution with a solid:liquid ratio of 2 g L^{-1}.[15] The suspension was shaken for 30 min at room temperature to release the nitrate ions adsorbed on the composite. The desorbed composite was then separated, washed to neutral pH and dried to a constant mass for subsequent experiments. The conditions of reusability evaluation were similar to the optimal adsorption conditions above.

3. Results and discussion

3.1. Effect of synthesis conditions on the properties of the composite

3.1.1. Effect of C : ZP weight ratio. The adsorption ability of the synthesized CZP composites at different C : ZP weight ratios was investigated under fixed adsorption conditions (pH 7, adsorbent dose of 1 g L^{-1}, nitrate concentration of 100 mg L^{-1} and contact time of 30 min). As shown in Fig. 2A, the AE and AC of CZP1, CZP2 and CZP3 corresponding to C : ZP weight ratios of 1 : 1, 1 : 2 and 1 : 3, respectively showed high values. This means that adding the chitosan component positively enhances the AE and AC compared to ZP. The maximum AE and AC values are 35.77% and 47.12 mg g^{-1} for CZP2, respectively. With the majority of ZP (CZP4 and CZP5), the nitrate adsorption ability insignificantly differs from that of ZP. A previous study reported that the composite based on zeolite A and chitosan also has a similar trend; with increasing chitosan content, the nitrate adsorption ability increased remarkably.[2] However, a further increase in chitosan did not lead to a noticeable enhancement in the AC of nitrate.

The variation in weight loss of chitosan, ZP, and the synthesized composites at different C : ZP weight ratios is presented in Table 1. Due to its organic nature and thermal degradation range between 200 and 500 °C,[16] chitosan exhibits the highest weight loss of 98.55% after calcination at 700 °C for 2 h. ZP, which comprised oxides such as SiO_2, Al_2O_3, and Na_2O,[12] revealed significantly lower weight loss compared to chitosan and the CZP composites. The weight loss of CZP composites (CZP1–CZP5) decreases progressively from 63.60% to 31.51%, demonstrating the compositional variation in

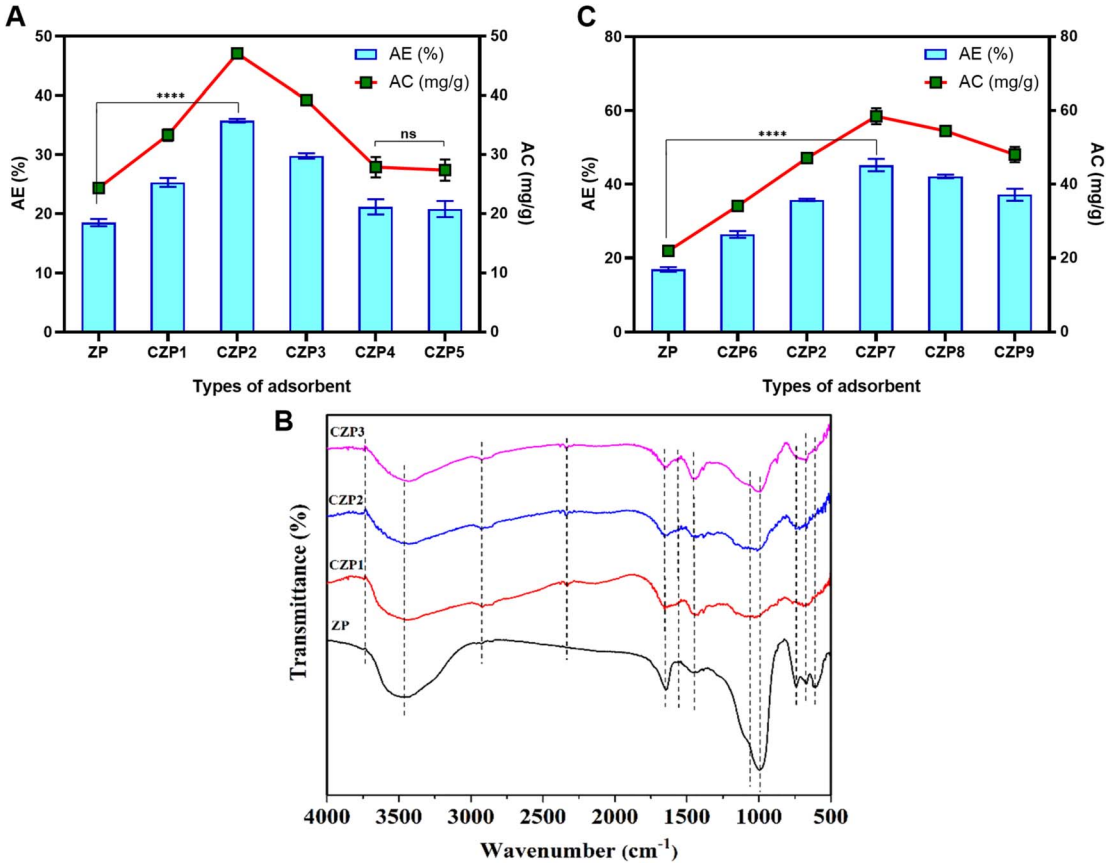

Fig. 2 Nitrate adsorption ability (A); FTIR results (B) of ZP and CZP synthesized at different weight ratios of C : ZP; and nitrate adsorption ability of ZP and CZP synthesized at various glutaraldehyde concentrations (C). Significance level ($p < 0.05$): ns means not significant and ****$p < 0.0001$.

Table 1 The weight loss of chitosan, ZP and CZP composites synthesized at varying weight ratios of C : ZP

Sample	Weight loss (%)
CTS	98.55 ± 0.29
ZP	16.21 ± 0.81
CZP1	63.60 ± 3.28
CZP2	45.94 ± 0.30
CZP3	40.55 ± 1.76
CZP4	35.21 ± 0.35
CZP5	31.51 ± 0.83

composites resulting from changes in the C : ZP weight ratio during the mixing stage.

Based on the results of adsorption and weight loss, CZP1, CPZ2 and CZP3 composites were selected for further analysis. The FTIR spectra of ZP, CZP1, CZP2, and CZP3 are shown in Fig. 2B and Table S2. The absorption band at 3477 cm^{-1} was attributed to O–H stretching vibrations associated with physically adsorbed water on the material surface,[2] while the band at 1647 cm^{-1} corresponds to O–H bending vibrations within the ZP framework.[17] Characteristic vibrations of the tetrahedral T–O–T (T = Si or Al) units in ZP were also observed at 993, 740, 669, and 608 cm^{-1}, respectively.[17] These characteristic bands of ZP were retained in composites, along with the integration of chitosan-related vibrations observed in CZP1 to CZP3. The bands in the range of 3744–3766 cm^{-1} demonstrated the presence of hydroxyl (–OH) groups from chitosan.[18] The C–H stretching vibrations were observed at 2921–2929 cm^{-1}, and the formation of cross-linking between chitosan and glutaraldehyde was evidenced by the presence of C=N stretching bands in the range of 2331–2341 cm^{-1}.[16] The N–H bending vibrations from chitosan were exhibited from 1530 to 1537 cm^{-1} while C–H bending vibrations were identified between 1422 and 1438 cm^{-1}.[12] The presence of ether linkages (C–O–C) was confirmed by bands at 1010–1030 cm^{-1}.[12] Generally, the characteristic vibration of both chitosan and ZP is noted in the CZP composites, and the influence of glutaraldehyde on the composite structure is also evident.

The properties of ZP and CZP1 and CZP2 composites were investigated through zeta potential measurements (Table 2). The zeta potential value of ZP is −91.1 mV, consistent with values reported in previous studies. This highly negative

Table 2 Zeta potential of ZP and CZP composites synthesized at different weight ratios of C : ZP

Sample	ZP	CZP1	CZP2
Zeta potential (mV)	−91.1	−56.9	−70.7

potential arises from its framework structure, which consists of negatively charged AlO_4^- and SiO_4^- tetrahedra.[19] Upon the incorporation of chitosan, the zeta potential of composites became significantly less negative. Specifically, the zeta potentials of CZP1 and CZP2 are −56.9 mV and −66.3 mV, respectively. This increase in zeta potential was attributed to the presence of chitosan, which was known to carry a positive surface charge.[20] The formation of CZP composites primarily involved electrostatic interactions between the negatively charged framework of ZP and the protonated $-NH_2$ groups of chitosan,[21] leading to a change in the zeta potential of composites. The same charge repulsion between the material surface and nitrate ions could negatively affect the nitrate adsorption; thus, the increased zeta potential helps mitigate this repulsion, enhancing the AC of nitrate.

3.1.2. Effect of glutaraldehyde concentration. The changes in AE and AC using the synthesized composites at different glutaraldehyde concentrations are illustrated in Fig. 2C. The adsorption conditions are at pH 7, an adsorbent dose of 1 g L^{-1}, a nitrate concentration of 100 mg L^{-1} and a contact time of 30 min. At all glutaraldehyde concentrations (1–8%), the AC and AE are higher than that of ZP. The AE and AC values gradually increase from CZP6 to CZP7, reaching the highest values for the CZP7 composite (45.23% and 58.49 mg g^{-1}). When the glutaraldehyde concentrations are further increased to 6% (CZP8) and 8% (CZP9), the AE and AC tended to decrease. To better understand the change in the composite properties, the weight loss of composites was also determined (Table 3). The weight loss of composites synthesized at different glutaraldehyde concentrations generally does not exhibit a remarkable difference. This demonstrates the stability of chitosan and ZP components in composites when changing the glutaraldehyde concentration.

The differences in AE and AC among composites can be explained based on their zeta potential values (Table 4). At a glutaraldehyde concentration of 1% (composite CZP6), the zeta potential was −77.9 mV. When the glutaraldehyde concentration is doubled and quadrupled, the zeta potential values increase to −70.7 mV (CZP2) and −66.3 mV (CZP7), respectively. The less negative values promote favorable interactions between the composite surface and nitrate ions, resulting in the enhancement of both AE and AC. However, excessive glutaraldehyde concentration provides a more negative zeta potential for CZP8 compared to composites synthesized with lower glutaraldehyde concentrations. Higher glutaraldehyde content reduced the positive surface charge of chitosan by decreasing the number of free NH_4^+ groups available.[22] As a result, it is essential to optimize the crosslinker concentration. In this study, the 4% glutaraldehyde concentration (CZP7), which exhibited the highest AE and AC, was identified as the optimal condition for the synthesis of CZP composites.

Table 3 The weight loss of chitosan, ZP and CZP composites synthesized at different glutaraldehyde concentrations

Sample	Weight loss (%)
CTS	98.55 ± 0.29
ZP	16.21 ± 0.81
CZP6	47.15 ± 2.27
CZP2	45.94 ± 0.30
CZP7	43.40 ± 0.98
CZP8	43.12 ± 0.47
CZP9	42.51 ± 0.39

Table 4 Zeta potential of ZP and composites synthesized at various glutaraldehyde concentrations

Sample	ZP	CZP6	CZP2	CZP7	CZP8
Zeta potential (mV)	−91.1	−77.9	−70.7	−66.3	−82.87

The XRD patterns of ZP and CZP7 can be found in Fig. 3A. The characteristic diffraction peaks of ZP can be observed at 2-theta angles of 12.68°, 17.89°, 21.67°, 28.10°, 30.84°, 33.38°, 35.76°, 38.01°, 46.08°, 51.12°, 52.89° and 54.66°. Upon the integration of chitosan, the characteristic peaks of ZP become less prominent due to the amorphous nature of chitosan, which tends to mask the crystalline reflections of ZP. Several characteristic peaks of ZP are still recorded in the CZP7 composite. The broad peaks at 2-theta angles of 10° and 20° exhibited the presence of chitosan in the composite.[23] From the above results, CZP composites are successfully synthesized with the main components including chitosan and ZP. In addition, energy dispersive spectroscopy (EDS) analysis of CZP, as illustrated in Fig. 3B, provides an enhanced characterization of the elemental composition of the material, thus confirming its crystalline morphology and structural consistency. The EDS spectrum identifies oxygen (O), carbon (C), aluminum (Al), silicon (Si), sodium (Na), and nitrogen (N), as the predominant elements, with respective weight percentages of 48.8%, 29.3%, 7.3%, 7.3%, 3.9%, and 3.4%, respectively. This compositional profile is consistent with the theoretical compositional ratio of CZP, based on the zeolite P (sodium–aluminum–silicon) framework and chitosan (carbon–oxygen–nitrogen). A final peak is characteristic of platinum, which was added to assist in the conductivity of the sample measurement. These spectral features confirm the presence of zeolite P and chitosan in CZP. SEM images of CZP7 (Fig. 3C) indicate that the composite surface with fairly uniform particles in size and shape, is characterized by pores and roughness. A similar morphology was previously observed in the case of zeolite X/chitosan and natural/chitosan.[13,24] Additionally, the numerous pores formed by the combination of ZP and chitosan also provide more active sites to improve the nitrate AC of the composite.

The point of zero charge (pH_{pzc}) of CZP7 is 7.8, which means that at pH < 7.8, CZP7 is positively charged and *vice versa*. At pH 4, AE and AC reach the highest values of 54.23% and 65.71 mg g^{-1}, respectively (Fig. 4A). As the pH value increases to 5, both AE and AC slightly decrease to 50.79% and 61.54 mg g^{-1}, and this trend continues reducing at pH 6. At pH 7, the electrostatic interactions between the composite surface and nitrate ions diminish due to a reduced charge differential. When the pH exceeds the pH_{pzc}, a noticeable decline in nitrate adsorption is

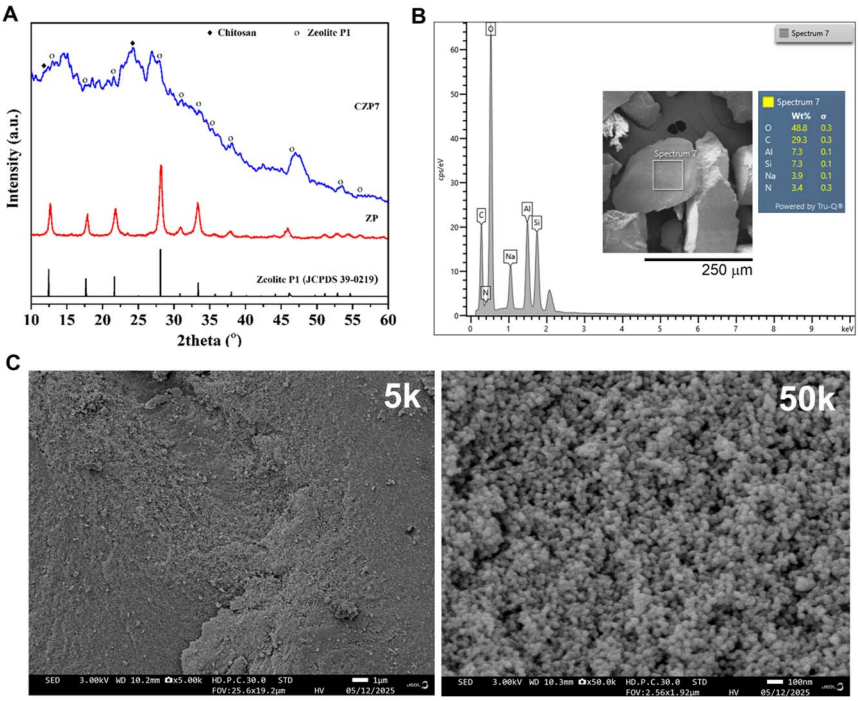

Fig. 3 XRD patterns of ZP and CZP7 (A) and SEM images at different magnifications of the CZP7 composite (B and C).

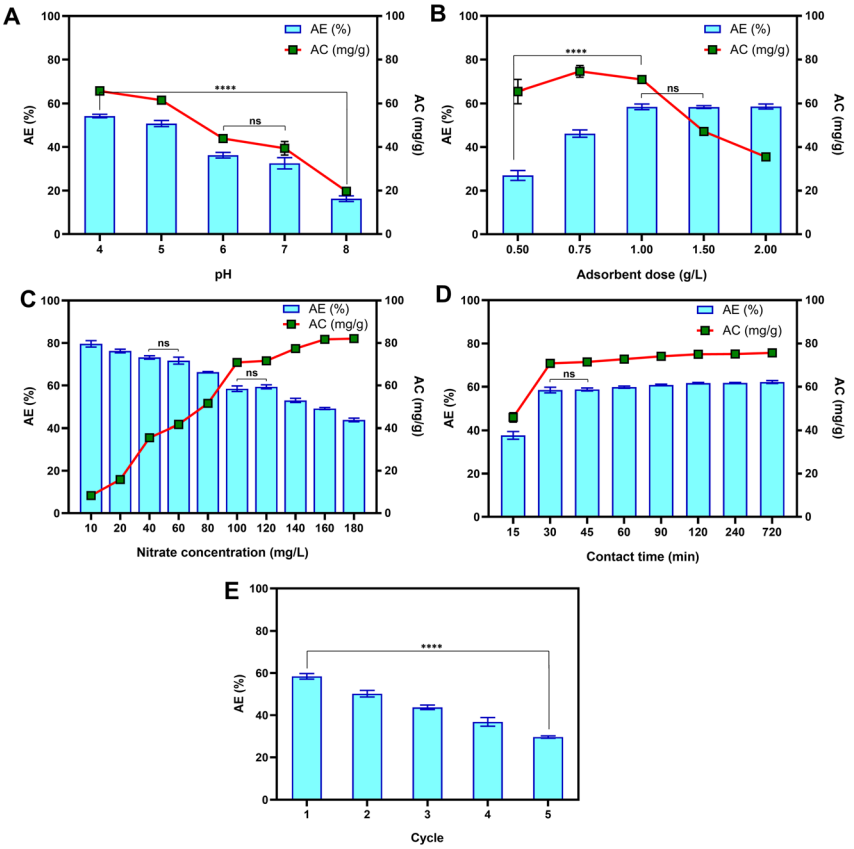

Fig. 4 Effects of pH (A); adsorbent dose (B); nitrate concentration (C); contact time (D) on the nitrate adsorption ability of CZP7 and the reusability of CZP7 (E). Significance level ($p < 0.05$): ns means not significant and ****$p < 0.0001$.

observed. This is evidenced by the lowest AE and AC values of 16.27% and 19.71 mg g^{-1} at pH 8, respectively. This tendency was also reported in previous studies. At pH values lower than the pH_{pzc}, the composite surface carried positive charges, creating favorable conditions for the nitrate adsorption.[20] As pH increased, the positive surface charge decreased, weakening the electrostatic interactions between the adsorbent and the nitrate ions, therefore reducing the AE.[25] In this study, pH 5 was selected as the optimal condition for further experiments because it provided the effective removal of nitrate. Moreover, pH 5 offers greater composite stability, as the ZP component of the composite is unstable under strongly acidic conditions.

3.2. Effect of operating conditions on the nitrate adsorption of the composite

Fig. 4B shows the nitrate AC of composites with different adsorbent doses (0.5–2.0 g L^{-1}). The efficiency gradually increases with increasing adsorbent dose from 0.5 to 1.0 g L^{-1} (26.98–58.47%). Further addition of adsorbent does not significantly change the efficiency (58.33–58.60%). Meanwhile, in the range of 0.5–1 g L^{-1}, ACs increase from 65.38 to 74.57 mg g^{-1}, and then decrease slightly to 70.83 mg g^{-1}. A marked decrease occurred at adsorbent doses of 1.5 and 2.0 g L^{-1}. The low AE values at adsorbent doses of 0.5 and 0.75 g L^{-1} were the result of a lack of active sites capable of adsorbing nitrate ions. With high doses, the abundance of adsorption sites promoted the interaction between the adsorbent and nitrate ions, leading to an increase in AE.[3,26] However, with an excess adsorbent dose, the AE does not increase significantly. The high AC values in the range of 0.5–1.0 g L^{-1} indicated dense coverage of nitrate ions on a small number of adsorption sites, indicating efficient utilization of the adsorbent. The excess number of active sites did not support the capture of nitrate ions and led to a decrease in AC. For that reason, to avoid wasting the adsorbent and ensure the AE, a dose of 1 g L^{-1} was selected for subsequent investigations.

Nitrate concentration is a critical factor influencing AE and AC of the CZP7 composite; therefore, a concentration range of 10–180 mg L^{-1} is investigated (Fig. 4C). The highest AE value of 79.63% is recorded at 10 mg L^{-1} and gradually reduces as the nitrate concentration increases from 20 to 180 mg L^{-1}. A slight decline in AE is observed within the range of 20–60 mg L^{-1}, while more decreases occur at concentrations above 80 mg L^{-1}. At 180 mg L^{-1}, the AE reaches the lowest value of 43.76%. Lower nitrate concentrations where most of the available adsorption sites could be fully utilized, result in high efficiency.[8] Conversely, at higher concentrations, the number of active sites became insufficient, leading to a decrease in AE. However, using excessive amounts of adsorbent under such conditions would be inefficient and wasteful. In contrast, AC increased with increasing nitrate concentration due to a higher amount of nitrate ions being captured per unit mass of adsorbent.[3] To balance AE and AC, the nitrate concentration of 100 mg L^{-1} was selected for further investigation of the effect of contact time.

The contact time is varied from 15 to 720 min to examine the effect of prolonging the time on the nitrate AC of the composite (Fig. 4D). In the first 15 min, AE and AC are 37.68% and 45.83 mg g^{-1}, respectively. When the contact time is doubled, AE and AC significantly increase to 58.47% and 70.83 mg g^{-1}, respectively. Further prolonging the contact time does not change the AE and AC values. As a whole, the CZP7 composite exhibits the nitrate adsorption ability in a short time and achieves the expected efficiency, indicating its potential application. The reusability of the CZP7 composite is also evaluated to consider its sustainability in practical applications (Fig. 4E). After the first cycle of adsorption and reuse, AE drops by about 5%. In the third adsorption cycle, AE continued to decrease by more than 10%, while AE reached 41.70% in the fourth usage cycle. After 5 uses, AE decreases by nearly 20% compared to the first adsorption.

Adsorption isotherm models are applied to investigate the mechanism of nitrate adsorption. The parameters of the Langmuir and Freundlich isotherm models are calculated based on the experimental data (Table 5). Both models exhibit

Table 5 Parameters of the isotherm models and the kinetic models

Isotherm models	Equations	Parameters	Values
Langmuir	$AC(mg\ g^{-1}) = \frac{(C_0 - C_e) \times V}{m}$ (3)	AC_{max} (mg g^{-1}): the Langmuir maximum adsorption capacity	107.761
		K_L (L mg^{-1}): the Langmuir adsorption equilibrium constant	0.037
		R^2	0.997
Freundlich	$AC_e = K_F C_e^{\frac{1}{n_F}}$ (4)	K_F (L g^{-1}): the Freundlich isotherm constant	10.992
		n_F: the constant related to the heterogeneity of the adsorbent surface	2.227
		R^2	0.952

Kinetic models	Equations	Parameters	Values
PFO	$AC_t = AC_e(1 - e^{-k_1 t})$ (5)	k_1 (1/min): the PFO rate constant	0.072
		AC_e (mg g^{-1}): the calculated AC	75.087
		R^2	0.999
PSO	$AC_t = \frac{k_2 AC_e^2 t}{1 + k_2 AC_e t_e}$ (6)	k_2 (g mg^{-1} min^{-1}): the PSO rate constant	0.002
		AC_e (mg g^{-1}): the calculated AC	79.600
		R^2	0.997

high correlation coefficients, with R^2 values of 0.997 (the Langmuir model) and 0.952 (the Freundlich model). However, due to the higher R^2, the Langmuir model provided a better fit for describing the nitrate adsorption behavior of the CZP composite, suggesting a monolayer adsorption process on a homogeneous surface.[27] The maximum adsorption capacity (AC_{max}) calculated from the Langmuir model is 107.761 mg g^{-1}, indicating the theoretical maximum uptake on a single layer of adsorbent. Moreover, the Freundlich model, despite its slightly lower correlation, still contributed insights into the adsorption mechanism. This model suggested a heterogeneous adsorption surface and implied interactions between adsorbed ions on the adsorbent surface.[28] Nitrate ions are unevenly distributed across the adsorption sites on the composite surface. The surface heterogeneity is further indicated by an n_F value of 2.227, which also reflects favorable adsorption behaviour. Generally, the nitrate adsorption process on the CZP7 composite involves both homogeneous and heterogeneous adsorption, with homogeneous adsorption being dominant as evidenced by the better fit of the Langmuir model.

The experimental data collected from the investigation of the effect of contact time are fitted with both PFO and PSO kinetic models. The R^2 values were 0.999 and 0.997 for PFO and PSO models, respectively indicating that the mechanism of nitrate adsorption on the composite could occur *via* both physical and chemical mechanisms.[3] The adsorption mechanism is mainly based on the electrostatic interaction between nitrate ions and the surface of CZP7. From the fit of the isotherm and kinetic models, it can be concluded that the nitrate adsorption process on the composite occurs favourably on a homogeneous surface with the important mechanism based on electrostatic interaction.

The adsorption mechanism is further clarified through FTIR spectra (Fig. 5). The composites before and after nitrate adsorption showed the characteristic vibration bands of ZP and chitosan suggesting that the CZP composite maintained its specific structural features after adsorption. For the post-adsorption CZP composite, a remarkable change appears in the wavenumber region below 1700 cm^{-1}, which is attributed to the interaction between nitrate ions and protonated $-NH_2$ groups under adsorption conditions at pH 5.[28] Meanwhile, a slight decrease in the intensity of vibrations in the range of 500–1000 cm^{-1} is mainly due to electrostatic interactions between the protonated ZP surface and anions.[10] Thus, the adsorption process predominantly occurs by a charge-sharing mechanism between the positively charged sites on the composite surface and nitrate ions (Fig. 5).

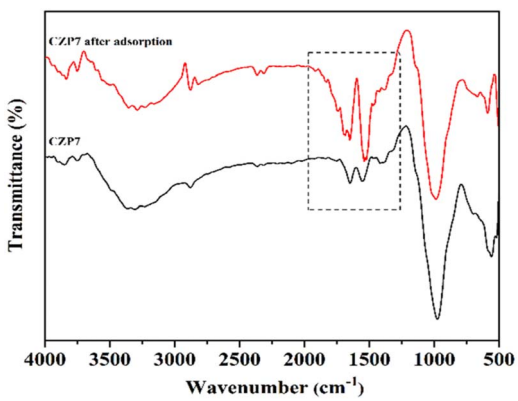

Fig. 5 The FTIR spectra of CZP7 and CZP7 after nitrate adsorption.

4. Conclusions

To control nitrate ion concentration in aquaculture and seafood processing systems, this study prepared CZP composites as an advanced material for efficient nitrate removal, contributing to sustainable water quality management. CZP composites, successfully synthesized with ZP derived from RHA, were developed from a cheap and readily available by-product to ensure economic viability. Characteristic vibrations of chitosan and ZP were fully exposed in the FTIR spectra. The mass loss of composites demonstrated the difference in their organic and inorganic components. Additionally, the significant increase in zeta potential values demonstrated the change in physico-chemical properties between ZP and composites. The morphology of composites was also characterized by voids and rough surfaces. Moreover, the nitrate adsorption of composites was investigated at pH 5, an adsorbent dose of 1 g L^{-1}, a nitrate concentration of 100 mg L^{-1} and a contact time of 30 min to achieve the optimal experimental AE and AC of 58.47% and 70.83 mg g^{-1}, respectively. The adsorption process indicated the good agreement with the Langmuir and Freundlich isotherm adsorption models with an R^2 of 0.997 and 0.952, respectively whereas AC_{max} based on the Langmuir model was 107.761 mg g^{-1}. The PFO (R^2 = 0.999) and PSO (R^2 = 0.997) models also described the adsorption mechanism of nitrate onto the composite well. The reusability of CZP was demonstrated with AE decreasing by about 20% after 5 uses. Therefore, the CZP composite is a potential material for application for wastewater treatment in the future.

Author contributions

N. T. N. Y.: project administration, supervision, and writing – review and editing; Y. N. N. T.: methodology; C. Q. N.: data curation, designing, and writing – review and editing; K. P. L.: methodology; writing – original draft; A. H. N.: methodology; N. M. N.: methodology; L. H. V. T.: methodology; Q. L. D.: methodology; Q. D. T.: methodology; P. L. T. N.: project administration. All authors have reviewed and approved the final draft.

Conflicts of interest

There are no conflicts to declare.

Data availability

The data supporting this article have been included as part of the supplementary information (SI). Supplementary information is available. See DOI: **https://doi.org/10.1039/d5su00593k**.

Acknowledgements

This research was funded by the Can Tho City Department of Science and Technology (CAST) under Decision no. 94/QĐ-SKHCN dated April 12th, 2024, and Contract no. 04/HĐ-SKHCN dated April 23rd, 2024. We thank Can Tho University of Technology and Can Tho University for providing lab facilities and equipment support.

References

1 X. Liu and L. Zhang, *Powder Technol.*, 2015, **277**, 112–119.
2 Y. Gao, Y. Ru, L. Zhou, X. Wang and J. Wang, *Adv. Compos. Lett.*, 2018, **27**, 185–192.
3 M. Nasir, F. Javaid, M. Talha Masood, D. Muhammad Arshad, M. Yasir, V. Sedlarik, M. Abdel Qadir, H. Qiblawey, W. Zhang, K. Mairaj Deen, E. Asselin and N. M. Ahmad, *Environ. Sci. Adv.*, 2024, **3**, 572–584.
4 Vietnam – the third largest seafood exporter in the world, **https://www.seafood.vasep.com.vn/why-buy-seafood/export-potentials/vietnam-the-third-largest-seafood-exporter-in-the-world-26061.html**, accessed April 28, 2025.
5 V. I. R. – VIR, Vietnam ranks among top three global shrimp exporters, **https://vir.com.vn/vietnam-ranks-among-top-three-global-shrimp-exporters-113391.html**, accessed April 28, 2025.
6 Vietnam's top 10 seafood export markets in Q1 2025, **https://vietfishmagazine.com/markets/vietnams-top-10-seafood-export-markets-in-q1-2025.html**, accessed April 28, 2025.
7 Developing the aquaculture sector from livable villages, **https://en.nhandan.vn/post-142850.html**, accessed April 28, 2025.
8 M. E. Ouardi, S. Qourzal, S. Alahiane, A. Assabbane and J. Douch, *J. Encapsulation Adsorpt. Sci.*, 2015, **5**, 178–190.
9 N. Y. Nguyen-Thi, C. Q. Nguyen, Q. L. Dang, Q. D. Tran, T. N. Do-Thi and L. H. V. Thanh, *RSC Adv.*, 2024, **14**, 4533–4542.
10 P. L. Tran-Nguyen, K.-P. Ly, T.-T. Nguyen, S. P. Santoso, N.-P.-D. Tran, A. E. Angkawijaya, M. Yuliana, M.-N. Nguyen and T. Thi-Tran-Anh, *J. Chem. Technol. Biotechnol.*, 2023, **98**, 1465–1477.
11 A. H. Jawad, A. S. Abdulhameed, A. Reghioua and Z. M. Yaseen, *Int. J. Biol. Macromol.*, 2020, **163**, 756–765.
12 L. Yu, J. Gong, C. Zeng and L. Zhang, *Mater. Sci. Eng., C*, 2013, **33**, 3652–3660.
13 L. G. de Araujo, V. Litrenta Medeiros, G. de Paula Guarnieri, D. A. da Silva, T. Watanabe, J. Takehiro Marumo and J. Geraldo Nery, *Environ. Sci. Adv.*, 2023, **2**, 484–494.
14 ISO 7890-3:1988,Water quality – Determination of nitrate, Part 3: Spectrometric method using sulfosalicylic acid.
15 A. Sowmya and S. Meenakshi, *Desalination Water Treat.*, 2014, **52**, 2583–2593.
16 S. V. Pawar and G. D. Yadav, *J. Mol. Catal. B: Enzym.*, 2014, **101**, 115–121.
17 P. Wang, Q. Sun, Y. Zhang and J. Cao, *Nano-Micro Lett.*, 2019, **14**, 572–576.
18 C. Schramm, *Spectrochim. Acta, Part A*, 2020, **243**, 118815.
19 C. Özel, C. Akat, R. Alosmanov, M. U. Kahveci, C. Emir and S. Yücel, *Bulg. Chem. Commun.*, 2021, **53**, 464–470.
20 F. C. Iswanti, I. Nurulita, S. Djauzi, M. Sadikin, A. B. Witarto and T. Yamazaki, *Biotechnol. Biotechnol. Equip.*, 2019, **33**, 390–396.
21 N. N. Safie, A. Zahrim Yaser and N. Hilal, *Asia-Pac. J. Chem. Eng.*, 2020, **15**, e2448.
22 C. J. Luk, Y. W. Yip, C. M. Yuen, C. W. Kan and K. Lam, *J. Fiber Bioeng. Inf.*, 2014, **7**, 35–52.
23 M. R. Abukhadra, M. Mostafa, M. N. B. Jumah, N. Al-Khalawi, R. S. Alruhaimi, Y. F. Salama and A. A. Allam, *J. Polym. Environ.*, 2022, **30**, 295–307.
24 G. T. Şanlı and E. Demirhan, *Biomass Convers. Biorefin.*, 2025, **15**, 3653–3662.
25 Y. Gao, S. Bao, L. Zhang and L. Zhang, *Desalination Water Treat.*, 2020, **203**, 160–171.
26 S. S. E. H. Elnashaie, F. Danafar and H. H. Rafsanjani, *Res. Dev. Mater. Sci.*, 2018, **6**, 1–11.
27 A. Rajeswari, A. Amalraj and A. Pius, *J. Water Proc. Eng.*, 2016, **9**, 123–134.
28 C. Chen, Y. Guo, L. Long, K. Chen, X. Hu and Y. Xue, *Environ. Sci. Pollut. Res.*, 2020, **27**, 32762–32769.